JACS
JOURNAL OF THE AMERICAN CHEMICAL SOCIETY
Article
pubs.acs.org/JACS

Multidentate Zwitterionic Ligands Provide Compact and Highly Biocompatible Quantum Dots

Naiqian Zhan, Goutam Palui, Malak Safi, Xin Ji, and Hedi Mattoussi*

Department of Chemistry and Biochemistry, Florida State University, 95 Chieftan Way, Tallahassee, Florida 32306, United States

Supporting Information

ABSTRACT: Hydrophilic functional semiconductor nanocrystals that are also compact provide greatly promising platforms for use in bioinspired applications and are thus highly needed. To address this, we designed a set of metal coordinating ligands where we combined two lipoic acid groups, bis(LA)-ZW, (as a multicoordinating anchor) with a zwitterion group for water compatibility. We further combined this ligand design with a new photoligation strategy, which relies on optical means instead of chemical reduction of the lipoic acid, to promote the transfer of CdSe-ZnS QDs to buffer media. In particular, we found that the QDs photoligated with this zwitterion-terminated bis(lipoic) acid exhibit great colloidal stability over a wide range of pHs, to an excess of electrolytes, and in the presence of growth media and reducing agents, in addition to preserving their optical and spectroscopic properties. These QDs are also stable at nanomolar concentrations and under ambient conditions (room temperature and white light exposure), a very promising property for fluorescent labeling in biology. In addition, the compact ligands permitted metal−histidine self-assembly between QDs photoligated with bis(LA)-ZW and two different His-tagged proteins, maltose binding protein and fluorescent mCherry protein. The remarkable stability of QDs capped with these multicoordinating and compact ligands over a broad range of conditions and at very small concentrations, combined with the compatibility with metal−histidine conjugation, could be very useful for a variety of applications, ranging from protein tracking and ligand−receptor binding to intracellular sensing using energy transfer interactions.

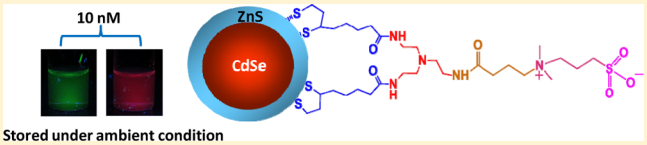

INTRODUCTION

The use of semiconductor nanocrystals (quantum dots) as fluorescent platforms to potentially improve our understanding of various complex biological processes has rapidly expanded in the past decade.[1−5] This has been motivated by their unique optical and spectroscopic properties combined with remarkable photo and chemical stability in comparison to other markers (e.g., organic dyes and fluorescent proteins).[6,7] Thus far, the preparation of high-quality QDs (with reduced size dispersity, crystalline cores, narrow emission profiles, and high photoemission quantum yields) has relied on the pyrolysis of organometallic precursors in hot coordinating solvents.[8−14] Overcoating the native core with a few monolayers of a wider band gap semiconducting material, such as ZnS, ZnSeS, and CdZnS, is also achieved using the high-temperature reaction route, albeit at temperatures slightly lower than what is used for the core growth. These materials are exclusively dispersible in organic solvents (e.g., hexane and toluene).[8,11,15−17] Thus, an additional surface-functionalization step is required to render them hydrophilic and biocompatible. Two main approaches have emerged as a means to achieve this goal. One uses encapsulation of the native QDs within an amphiphilic block copolymer or phospholipid micelles, while the other involves exchanging the native organic coat with a hydrophilic ligand shell (i.e., ligand or cap exchange).[18−27] Ligand exchange is easy to implement and can provide more compact nanocrystals. It can also permit the introduction of specific functionalities on the QD surface for further modifications using tailor-made capping molecules.[18,28−30]

Regardless of the strategy employed, successful integration of these quantum dots into biology (including whole-animal and cellular imaging) requires the availability of nanocrystals that exhibit a few important characteristics: (i) high quantum yield, (ii) long-term colloidal stability over a broad pH window and in the presence of elevated electrolyte concentrations, (iii) reduced nonspecific interactions with plasma and growth media proteins, and (iv) easy to tailor surface functionalities to introduce biomolecules through either covalent coupling and/or His-conjugation chemistry.[31−34] With the ligand exchange strategy, these requirements can be addressed using a rational ligand design.

Dihydrolipoic acid (DHLA) was one of the earlier ligands used where the stronger affinity to ZnS-overcoated QDs promoted by the higher coordination of the dithiol group was beneficial, as QDs with extended colloidal stability were prepared.[35] This ligand provides hydrophilic nanocrystals with a small hydrodynamic size.[36] However, due to the protic nature of the carboxy group, dispersions of DHLA-QDs aggregate under acidic conditions, and they exhibit nonspecific interactions in growth media.[35,37] One approach to address pH stability relied on introducing short polyethylene glycol segments either grafted onto lipoic acid or combined with

Received: May 18, 2013
Published: August 15, 2013

   dx.doi.org/10.1021/ja405010v | J. Am. Chem. Soc. 2013, 135, 13786−13795

Synthetic Scheme

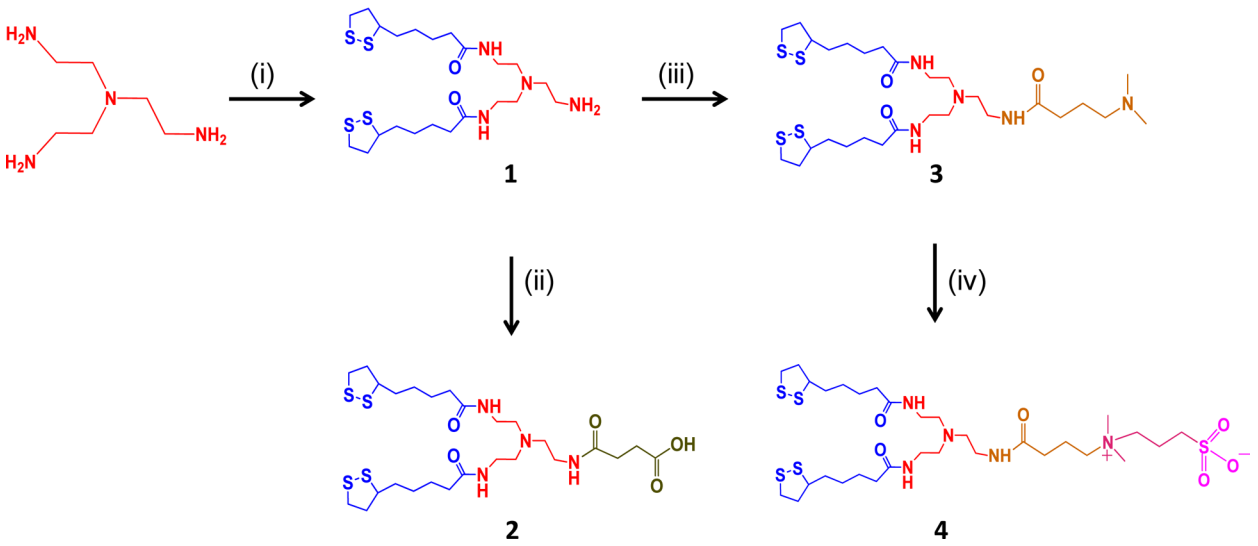

Figure 1. Chemical structures along with the synthetic steps used to prepare the targeted ligands. Reagents and conditions: (i) LA (lipoic acid), CDI (1,1′-cabonyldiimidazole); (ii) succinic anhydride, Et_3N; (iii) *N*,*N*-dimethylaminobutyric acid hydrochloride, Et_3N, DCC (*N*,*N*′-dicyclohexylcarbodiimide), DMAP (4-dimethylaminopyridine); (iv) 1,3-propanesultone, room temperature.

DHLA into larger polymer structures.[18,28,29,38−40] An alternative route that can provide compact nanocrystals with expanded pH stability can rely on the introduction of zwitterionic groups.[32,41,42]

Here we report the synthesis of a new set of multicoordinating zwitterion ligands that contain two dithiolane groups for enhanced affinity to the QD surface, along with one sulfobetaine moiety that promotes water solubility (Figure 1). This route also provided bis(LA) ligands that present either a terminal amine or a carboxyl group. This design builds on previous work where the presence of four thiols attached to a single PEG chain was shown to provide remarkable long-term colloidal stability to QDs and Au nanoparticles.[39] We further combine the ligand design with a photoligation strategy to promote nanocrystal phase transfer under borohydride-free conditions. This approach has provided a set of compact hydrophilic QDs that exhibit excellent stability over a broad range of conditions, including acidic and basic buffers, high electrolyte concentration, the presence of a biogenic thiol molecule (such as glutathione, GSH), and storage at very low concentrations, room temperature and with white light exposure. It has also allowed the insertion of reactive groups (either amine or carboxy) on the QD surface for further functionalization with biomolecules.[43] The compactness of the ligand is further demonstrated by conjugating the QDs to proteins expressing terminal polyhistidine tags, via metal−His interactions, which involves direct coordination between the imidazoles and the Zn-rich surface of the QDs.

EXPERIMENTAL SECTION

Materials. All synthetic reactions described here were carried out under a nitrogen atmosphere, unless otherwise specified; air-sensitive materials were handled in an MBraun Labmaster 130 glovebox (Stratham, NH). Lipoic acid (LA), *N*,*N*-dimethylaminobutyric acid hydrochloride, *N*,*N*′-dicylohexylcarbodiimide (DCC), 1,1′-carbonyldiimidazole (CDI), 4-dimethylaminopyridine (DMAP), triethylamine, tetramethylamonium hydroxide (TMAH), folic acid, and organic solvents (chloroform, methanol, hexane, etc.) were purchased from Sigma Chemicals (St. Louis, MO). Phosphate salts used for buffer preparation, NaCl, Na_2CO_3, and Na_2SO_4 were also purchased from Sigma Chemicals. Tris(2-aminoethyl)amine and 1,3-propanesultone were purchased from Alfa Aesar (Ward Hill, MA). Column chromatographic purification was performed using silica gel (60 Å, 230−400 mesh, from Bodman Industries, Aston, PA). Deuterated solvents used for NMR experiments were purchased from Cambridge Isotope Laboratories (Andover, MA). D-(+)-Maltose hydrate and amylose resin were purchased from Sigma Chemicals and New England Biolabs Inc. (Ipswich, MA), respectively. Monoreactive *N*-hydroxysulfosuccinamide (sulfo-NHS)-Cy3 dye and PD10 columns were purchased from GE Healthcare (Piscataway, NJ). The chemicals and solvents were used as received unless otherwise specified.

Instrumentation. The ^{1}H NMR spectra were collected using a Bruker SpectroSpin 600 MHz spectrometer, while Fourier transform infrared (FT-IR) spectra were recorded on a Perkin-Elmer FT-IR spectrometer. A JEOL AccuTOF JMS-T100LC ESI mass spectrometer (ESI-MS) was used to determine the mass of the ligands. A Shimadzu UV−vis absorption spectrophotometer (UV 2450 model) was used to measure the UV−vis absorption spectra from the various dispersions, while the fluorescence spectra were collected on a Fluorolog-3 spectrometer (Jobin Yvon Inc., Edison, NJ) equipped with PMT and CCD detectors. Solvent evaporation (to concentrate or dry samples) was carried out using a lab-scale Buchi R-215 rotary evaporator (New Castle, DE). The photoligation experiments were carried out using a UV photoreactor, Model LZC-4 V (Luzchem Research Inc., Ottawa, Canada). Dynamic light-scattering measurements were performed using an ALV/CGS-3 Compact Goniometer System equipped with an avalanche photodiode for signal detection and ALV photon correlator, and the resulting autocorrelation function was fitted to a cumulant series using ALV-7004 correlator software.[36] Additional details are provided in the Supporting Information. Gel electrophoresis experiments were run on a 1% agarose gel. The dispersions of QDs or QD-conjugates were first diluted in a TBE, tris borate EDTA (100 mM Tris, 83 mM boric acid, 1 mM EDTA, pH 8.4) mixed with ficoll 400 loading buffer. Aliquots of these dispersions were loaded into the agarose gel and run for 20 min using an applied voltage of 8.0 V/cm. The gel was imaged using a UVP trans-illuminator equipped with a digital camera.

dx.doi.org/10.1021/ja405010v | J. Am. Chem. Soc. 2013, 135, 13786−13795

Ligand Synthesis. The new ligand made of a sulfobetaine zwitterion appended with two lipoic acid anchoring groups was prepared by starting from tris(2-aminoethyl)amine and applying a few simple reaction steps. First, two out of the three amine groups on tris(2-aminoethyl)amine were reacted with 2 equiv of lipoic acid. The remaining amine was then reacted with 1 equiv of *N,N*-dimethylaminobutyric acid moiety, followed by modification with 1,3-propanesultone, to yield the final bis(LA)-ZW, as indicated in Figure 1. In addition, two additional ligands were prepared: one was an amine-terminated species made from the intermediate bis(LA)-NH_2 and the other was prepared following transformation of the amine to COOH using succinic anhydride to provide bis(LA)-COOH. These ligands were applied for the photoligation of TOP/TOPO-QDs. We will briefly describe the synthetic steps used to prepare these various compounds.

Compound 1 (N,N′-(((2-Aminoethyl)azanediyl)bis(ethane-2,1-diyl))bis(5-(1,2-dithiolan-3-yl)pentanamide), bis(LA)-NH_2). In a 250 mL three-neck round-bottom flask lipoic acid (5.0 g, ∼24.27 mmol) and 1,1′-carbonyldiimidazole (CDI) (4.3 g, ∼26.5 mmol) were mixed and purged with N_2 for 10 min. Chloroform (40 mL) was added via a syringe, and the solution was stirred for 2 h at room temperature under a nitrogen atmosphere until fully homogenized. This yellow solution was transferred to an addition funnel, which was mounted onto a second round-bottom flask, and the contents were slowly added (dropwise) to a solution containing tris(2-aminoethyl)amine (1.5 mL, ∼10.02 mmol) dissolved in 40 mL of chloroform, and this mixture was stirred for 2 days. The reaction mixture was transferred to a separating funnel and washed with water (30 mL, two times) and then with saturated sodium carbonate (30 mL, three times) to remove excess uncoupled lipoic acid. The chloroform layer was washed with brine, dried over Na_2SO_4, concentrated, and then chromatographed on a silica column (230−400 mesh). The latter was implemented in two steps: first, the organic impurities were removed using a lower percentage of a methanol mixture, followed by elution using a higher polarity mixture of chloroform/methanol (5/1). This procedure yielded compound **1** (∼2.0 g, ∼35% yield). The ^{1}H NMR spectrum of compound **1** is shown in the Supporting Information (Figure S1).

Note: one should not excessively dry the sample (under vacuum), as the very dry compound is difficult to dissolve in chloroform, which can eventually complicate the next step(s).

^{1}H NMR (600 MHz, DMSO-d_6): δ 7.80 (t, 2H, J = 5.5 Hz), 3.62−3.59 (m, 2H), 3.22−3.16 (m, 2H), 3.15−3.10 (m, 2H), 3.10−3.05 (m, 2H), 2.53−2.49 (m, 2H), 2.47−2.37 (m, 7H), 2.12−2.05 (t, 4H, J = 7.4 Hz),1.91−1.82 (m, 2H), 1.88−1.85 (m, 2H), 1.58−1.48 (m, 6H), 1.4−1.31 (m, 4H). IR (neat): 3237.80, 3075.39, 2924.6, 2853.17, 1633.25, 1542.07, 1458.84, 1458.84, 1433.03, 1355.72 cm^{-1}. ESI-MS (m/z): calcd for $C_{22}H_{42}N_4O_2S_4$ $(M + H)^+$ 523.3, found 523.2.

Compound 2 (4-((2-(Bis(2-(5-(1,2-dithiolan-3-yl)pentanamido)ethyl)amino)ethyl)amino)-4-oxobutanoic acid, bis(LA)-COOH). Compound **1** (∼0.52 g, 0.93 mmol) dissolved in chloroform (40 mL) was placed in a 100 mL round-bottom flask equipped with a stirring bar. Succinic anhydride (1.92 g, 1.92 mmol) and triethylamine (0.27 mL, 1.92 mmol) were added to the solution followed by purging with nitrogen. After it was stirred overnight, the reaction mixture was washed with water (30 mL, two times), dried over Na_2SO_4, concentrated (using rotary evaporator), and then chromatographed on a silica column (230−400 mesh) using a chloroform/methanol mixture (6/1) as the eluent; this procedure yielded compound **2** (0.3 g, ∼50% yield) as a solid. The ^{1}H NMR spectrum of compound **2** is shown in the Supporting Information (Figure S2).

^{1}H NMR (600 MHz, DMSO-d_6): δ 7.81 (t, 1H, J = 5.2 Hz), δ 7.74 (t, 2H, J = 5.2 Hz), 3.64−3.57 (m, 2H), 3.22−3.16 (m, 2H), 3.15−3.1 (m, 2H), 3.15−3.04 (m, 6H), 2.49−2.44 (m, 6H), 2.44−2.37 (m, 4H), 2.3 (t, 2H, J = 7.0 Hz), 2.09 (t, 4H, J = 7.4 Hz), 1.89−1.84 (m, 2H), 1.70−1.64 (m, 2H), 1.58−1.51 (m, 6H), 1.38−1.31 (m, 4H). IR (neat): 3297.61, 3079.36, 2924.60, 2853.17, 1768.06, 1694.71, 1637.22, 1532.15, 1431.05, 1403.03 cm^{-1}. ESI-MS (m/z): calcd for $C_{26}H_{46}N_4O_5S_4$ $(M)^+$ 622.2, found 622.3.

Compound 3 (N,N′-(((2-(4-(Dimethylamino)butanamido)ethyl)azanediyl)bis(ethane-2,1-diyl))bis(5-(1,2-dithiolan-3-yl)pentanamide), bis(LA)-N,N-dimethyl alkyl amide). In a 100 mL round-bottom flask *N,N*-dimethylaminobutyric acid hydrochloride (0.72 g, 4.3 mmol) and triethylamine (0.665 mL, 4.73 mmol) were dissolved in chloroform (30 mL) and the solution was stirred for 30 min. DCC (0.59 g, 2.87 mmol) and a catalytic amount of DMAP were added to the reaction mixture, which was stirred for 30 min under ice-cold conditions. Compound **1** (1.5 g, 2.87 mmol) dissolved in chloroform (40 mL) was slowly added to the flask, and the reaction mixture was stirred for 2 days under a nitrogen atmosphere. Dicyclohexylurea (DCU) was removed by filtration, and the chloroform layer was further washed with saturated sodium carbonate solution (30 mL, two times) to remove excess unreacted *N,N*-dimethylaminobutyric acid. The solution was concentrated and then purified on a silica column (230−400 mesh) using a chloroform/methanol mixture (6/1) as the eluent to isolate the compound **3** (1.19 g, ∼65% yield). The ^{1}H NMR spectrum of this compound is shown in the Supporting Information (Figure S3).

^{1}H NMR (600 MHz, DMSO-d_6): δ 7.72 (t, 3H, J = 5.5 Hz), 3.64−3.57 (m, 2H), 3.22−3.16 (m, 2H), 3.15−3.10 (m, 2H), 3.10−3.05 (m, 6H), 2.46 (t, 6H, J = 6.5 Hz), 2.44−2.38 (m, 2H), 2.18−2.16 (t, 2H, J = 7.2 Hz), 2.10 (s, 6H), 2.10−2.07 (t, 6H, J = 7.6 Hz), 1.9−1.83 (m, 2H), 1.7−1.63 (m, 2H), 1.64−1.59 (m, 2H), 1.57−1.47 (m, 6H), 1.4−1.30 (m, 4H). IR (neat): 3273.80, 3087.3, 2932.53, 2825.39, 1635.24, 1546.03, 1446.91, 1377.53 cm^{-1}. ESI-MS (m/z): calcd for $C_{28}H_{53}N_5O_3S_4$ $(M + H)^+$ 636.3, found 636.3.

Compound 4 (12-(2-(5-(1,2-Dithiolan-3-yl)pentanamido)ethyl)-20-(1,2-dithiolan-3-yl)-4,4-dimethyl-8,16-dioxo-4,9,12,15-tetraazaicosan-4-ium-1-sulfonate, bis(LA)-zwitterion). In a 50 mL round-bottom flask, compound **3** (1.0 g, 1.57 mmol) was dissolved in 20 mL of $CHCl_3$, followed by dropwise addition of 1,3-propanesultone (0.165 mL, 1.88 mmol). This reaction mixture was purged with nitrogen and stirred for 3 days at room temperature, yielding a clear yellow solution of compound **4**, which was characterized by ^{1}H NMR and mass spectroscopy (see the Supporting Information, Figures S4 and S5). A slight excess of 1,3-propanesultone was used to ensure complete transformation of compound **3**. The product (compound **4**) was isolated by evaporation of the chloroform, yielding 1.5 g of product (or a reaction yield of ∼100%). We should note that no further purification of compound **4** was carried out, because the impurities (essentially excess unreacted sultone) do not interfere with the photopromoted ligation of the QDs (see below); unreacted sultone exhibits no affinity to the QD surfaces. Indeed, we found that once photopromoted ligand exchange was complete, the sultone impurities could be easily removed during the purification step. The ligand (compound **4**) was stored in $CHCl_3$ for future use. This is rather important, as redispersion of the ligand molecule in organic solvent after excessive drying becomes difficult.

IR (neat): 3404.76, 3289.68, 3087.30, 2928.57, 2857.14, 1641.18, 1540.08, 1452.86, 1339.88, 1254.62, 1163.43, 1036.57, 959.25 cm^{-1}. ESI-MS (m/z): calcd for $C_{31}H_{59}N_5O_6S_5$ $(M + H)^+$ 758.3, found 758.3.

Quantum Dot Synthesis. CdSe-ZnS core−shell QDs were synthesized by reacting organometallic precursors (e.g., cadmium acetylacetonate and trioctylphosphine selenium, TOP:Se) in two steps, as described in previous reports.[9,13,44] The first allows the growth of the CdSe cores, followed by overcoating with a thin ZnS layer in the second step, usually carried out at slightly lower temperature.[10,11,13,15,17] As-prepared QDs primarily capped with TOP/TOPO were mixed with a small fraction of alkylamine and alkylcarboxy ligands, which makes them highly hydrophobic and dispersible only in organic solvent (e.g., toluene or hexane). The native cap on the hydrophobic nanocrystals is exchanged with hydrophilic ligands to promote water solubility and biological reactivity.[18,45]

Photoligation of the Quantum Dots. The ligand exchange was carried out using a photoligation strategy, where the native TOP/TOPO-capped nanocrystals were irradiated with UV light at 350 nm in the presence of the oxidized form of the ligands (namely, bis(LA)-ZW).[43] We briefly describe the steps involved for capping the QDs with compound **4**. TOP/TOPO-capped CdSe-ZnS quantum dots (74 μL from a 17.6 μM stock solution) were first precipitated from a toluene/hexane mixture using ethanol and then redispersed in 500 μL

of hexane. Separately, 250 μL of a freshly prepared solution of compound **4** in $CHCl_3$ (containing 41 mg of bis(LA)-ZW) was loaded into a scintillation vial, the solvent was evaporated under vacuum, and then 550 μL of methanol was added. The mixture was stirred for 2 h, producing a homogeneous solution of bis(LA)-ZW ligand in methanol. A catalytic amount of tetramethylammonium hydroxide (TMAH, ∼20 mM) was added to facilitate the dissolution of the bis(LA)-ZW in methanol and to improve the effectiveness of the photoligation procedure. A slight heating (at 50−60 °C) can be used to speed up the dissolution of the ligands. These two solutions were combined in one vial, which was then sealed and the atmosphere switched to nitrogen. The vial containing the reaction mixture was placed inside a UV reactor (Model LZC-4 V, Luzchem Research, Inc., Ottawa, Canada) and irradiated for 60 min (λ_{irr} maximum peak at 350 nm, 4.5 mW/cm^2) with vigorous stirring. This produces macroscopic precipitation of the QD materials on the vial walls, indicating that the native TOP/TOPO ligands have been replaced with the new ligand, as described in our previous reports.[43] Precipitation was due to alteration of the solubility of the QD-plus-ligand in comparison to ligand alone or QD alone. The clear solution phase containing excess ligand and displaced TOP/TOPO was removed using a glass pipet, and the precipitate was washed with methanol (2 times, with centrifugation after each wash) to remove excess free bis(LA)-ZW and TOP/TOPO ligands. After an additional drying step under vacuum (for 1−2 min), DI water (or buffer) with a small amount of TMAH/NaOH was added to obtain a homogeneous dispersion of QDs; sonication of the sample for a few minutes could accelerate the nanocrystal dispersion in the media. At this step, the base is needed to circumvent the difficulties associated with the protonation of the tertiary nitrogen present in the molecule. Finally three to four rounds of concentration/dilution using a membrane filtration device (Amicon Ultra, 50 kD) were applied to provide a colloidal dispersion of bis(DHLA)-ZW-QDs in water. A similar procedure was applied to prepare amine- or carboxy-functionalized QDs. Here a mixture of bis(LA)-ZW and bis(LA)-NH_2 or bis(LA)-COOH (instead of pure bis(LA)-ZW) at the desired molar fraction was used for the photoligation procedure.

Protein Expression. We used two distinct proteins, maltose binding protein (MBP) and mCherry protein, which were appended at the N-terminus with 7-histidine and 6-histidine tags, respectively. The proteins were expressed in *E. coli* (*Escherichia coli*) bacteria (BL21 cells) starting from pMalE3 and pBAD plasmids for MBP and mCherry, respectively. Expression was induced using isopropyl β-D-1-thiogalactopyranoside for MBP and arabinose for mCherry. Both proteins were purified on a column loaded with a high-capacity nickel-IMAC resin (Ni-NTA, Fisher Scientific), and concentrations were determined by measuring the absorption at 280 nm for MBP and a combination of absorptions at 280 and 587 nm for mCherry. Additional details are provided in the Supporting Information

Self-Assembly of Quantum Dot-Bioconjugates. MBP-His_7 was self-assembled on the QDs photoligated with bis(LA)-ZW at varying average ratios of proteins per QD, depending on the final use of the conjugates. The QDs and protein were mixed in 10 mM pH 8 PBS buffer and left to react for 45 min. The QD-MBP conjugate formation was tested using QD PL enhancement upon assembling an increasing number of proteins per QD-conjugate and affinity chromatography, i.e. binding onto an amylose loaded column followed by release with added maltose, as done in our previous reports.[35,46] Self-assembly of QD-mCherry conjugates was carried out using a similar protocol. In a typical preparation, 30 μL aliquots of bis(LA)-ZW-QDs (∼3.23 μM stock solution) were added each to an Eppendorf tube containing 70 μL of 10 mM PBS buffer (pH 8). In separate Eppendorf tubes, varying amounts of His_6-appended mCherry solutions (starting from 11.4 μM stock solution) were mixed with PBS buffer. The mCherry solutions were then added to the dispersions of bis(LA)-ZW-QDs above. The volumes of buffer and solutions were adjusted to maintain a total final volume for the mixture equal to 400 μL with a QD concentration of ∼0.2 μM, while varying the molar ratio QD:mCherry from 1:3 to 1:15. The samples were incubated at 4 °C for ∼45 min to allow conjugate self-assembly, and then absorption and emission spectra for all samples were measured to characterize the binding and FRET interactions in these samples.

RESULTS AND DISCUSSION

Ligand Design. The design and synthesis of the new bis(LA)-ZW, bis(LA)-NH_2, and bis(LA)-COOH ligands is motivated by three goals: (i) the presence of two lipoic acid anchoring groups provides a stronger coordination onto the QDs, due to the multidentate chelating interactions with the semiconductor surfaces,[18,20,28,35,39,40] (ii) the zwitterion moiety bearing a sulfobetain group promotes aqueous solubility over a broad pH range, and (iii) the zwitterion-modified ligands are molecular scale and should provide QDs with small hydrodynamic size and a thin hydrophilic coating. The last point can permit access of a His tag to the QD surface for direct metal−histidine coordination, facilitating QD-protein self-assembly. The synthetic protocol for this set of ligands is simple and involved three straightforward steps: first, two lipoic acid moieties were coupled to two of the three amine groups of the tris(2-aminoethyl)amine using a CDI condensation strategy; a stoichiometric ratio was maintained for the selective coupling of two amine groups out of three. In the second step, *N*,*N*-dimethylaminobutyric acid was coupled to the remaining amine group of the core compound through amide bond formation using a DCC condensation reaction. Ring opening of the 1,3-propanesultone coupled with its reaction with the *N*,*N*-dimethyl moiety produced the bis(LA)-zwitterion ligand in the final step. The purification relied on (column) silica gel chromatography. The synthetic routes also allowed the preparation of two terminally reactive ligands, bis(LA)-NH_2 (an intermediate to bis(LA)-ZW) and bis(LA)-COOH.

Photoligation and Optical Characterization of the QDs. The ligand exchange was carried out using a strategy relying on the in situ reduction of the lipoic acid terminated ligands in the presence of the hydrophobic QDs using UV irradiation.[43] This photoligation strategy eliminates the need for the chemical reduction of the dithiolane group (on the lipoic acid, via $NaBH_4$) and has been found to effectively work with an array of ligands including pure LA, LA-PEG, and LA-zwitterion.[43] Furthermore, this approach is more advantageous when cap exchange is implemented using zwitterion modified mono- and bis-lipoic acid ligands, because preparation and purification of the chemically reduced form of the ligands is rather difficult.[46]

We have applied this strategy to cap TOP/TOPO-QDs with the three ligands described above (see Figure 1): bis(LA)-ZW and mixtures of bis(LA)-ZW and bis(LA)-NH_2 and of bis(LA)-ZW and bis(LA)-COOH. In our previous reports, we have shown that UV irradiation of a solution of the pure ligand induces a progressive decrease in the disulfide absorption signature (peak at ∼340 nm), which we attributed to the transformation of the lipoic acid (LA) into an intermediate diradical.[43] When irradiation is carried out in the presence of the QDs, these intermediate ligands interact with the photoexcited QDs, leading to in situ replacement of the TOP/TOPO with the new ligand and the ensuing phase transfer.

Here, the photoligation procedure was carried out using a two-phase reaction, where prior to UV exposure the native TOP/TOPO-QDs were dispersed in hexane (nonpolar phase), while the bis(LA)-ZW ligand was dissolved in methanol (polar phase) containing TMAH base. We found that UV irradiation consistently resulted in the complete precipitation of the QD

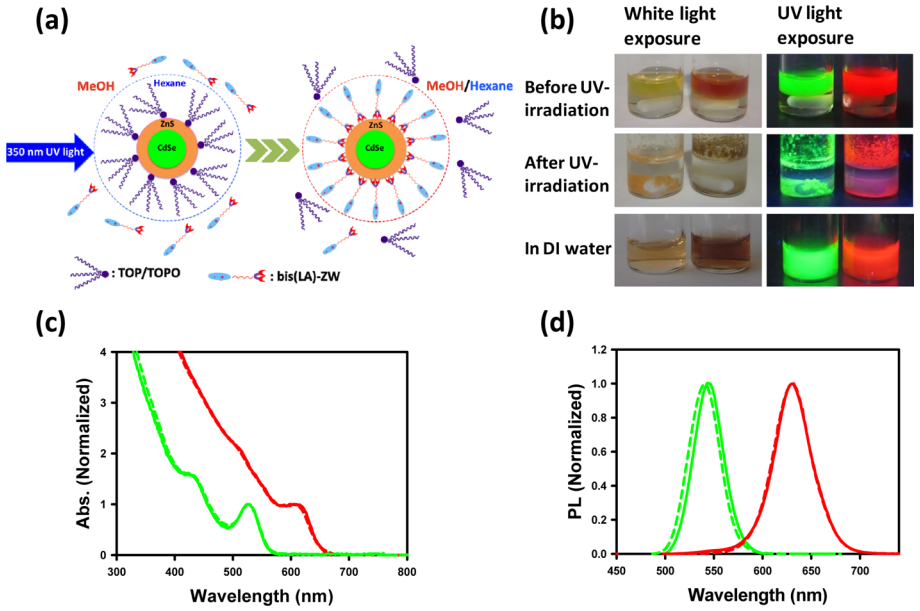

Figure 2. (a) Schematic representation of the photoligation strategy. (b) White light and fluorescence images of dispersions of two different size QDs, before and after photoirradiation. The corresponding dispersions in water are also shown at the bottom. (c) UV−vis absorption and (d) PL spectra of the two QD samples (λ_{em} = 540 and 624 nm). Dotted lines represent hydrophobic QDs in organic solvents, and solid lines correspond to the hydrophilic QDs following photoligation using bis(LA)-ZW. The absorption and PL spectra were normalized with respect to the band edge peak and the emission maximum, respectively.

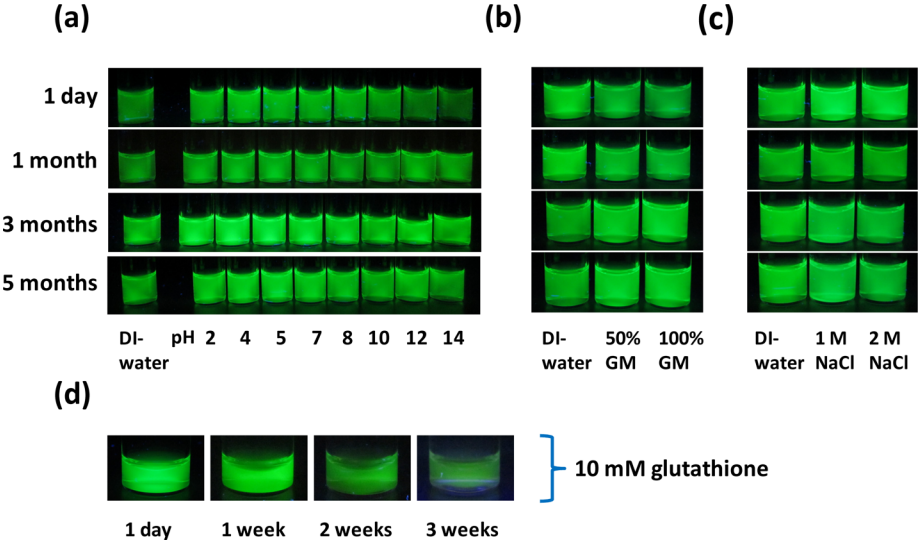

Figure 3. Fluorescence images of dispersions of QDs photoligated with bis(LA)-ZW (0.5 μM) at different storage times: (a) in phosphate buffer (~20 mM) at pH ranging from 2 to 14; (b) in the presence of 50% and 100% RPMI growth media (GM); (c) in the presence of 1 and 2 M NaCl. (d) Fluorescence images of QD dispersions containing 10 mM glutathione (GSH).

materials. Following removal of the supernatant solvents, washing with methanol, and gentle drying, the nanocrystals were readily dispersible in DI water (Figure 2). We successfully applied this photoligation strategy to phase transfer a series of different size QDs; a representative set is shown in Figure 2b for green- and red-emitting QDs (λ_{em} 540 and 624 nm). Figure 2c,d shows that the normalized absorption and emission spectra of two sets of QDs in organic solvents (TOP/TOPO-capped QDs) and in water after photoligation were essentially identical. Thus, the new bis(LA)-ZW ligand combined with the photoligation technique did not alter the photophysical properties of the nanocrystals, as reported for other LA-based ligands.[43] We should, however, note that the phase transfer to water was accompanied by a loss of the PL quantum yield in comparison to the native materials. For instance, the quantum yields measured for the hydrophilic QD dispersions are 30−50% smaller than those measured for TOP/TOPO-QDs in hexane (i.e., ~30−50% loss); the exact value of the measured quantum yield may vary depending on the quality of the zinc sulfide shell, which is consistent with our previous data.[43]

Colloidal Stability of the Hydrophilic QDs. The colloidal stability of QDs photoligated with bis(LA)-ZW ligands in water was tested under a few representative conditions: with pH changes, in the presences of excess added NaCl, in cell growth media, in the presence of 10 mM glutathione, and with storage in pH 7 PBS buffer under the conditions of very low

dx.doi.org/10.1021/ja405010v | J. Am. Chem. Soc. 2013, 135, 13786−13795

concentrations (10, 50, and 100 nM) combined with room temperature and light exposure.

These stability tests are important, as they can indicate the ability of the hydrophilic nanocrystals to perform targeted sensing or imaging in biological media, which are rich in electrolytes and reducing agents. Indeed, glutathione concentration in the cytosol of live cells can be as high as 10 mM.[47,48] Colloidal stability at very low concentrations and with room temperature and light exposure could provide an idea about the strength of the ligand binding to the nanocrystal at the concentrations needed for intracellular tracking and sensing experiments. For instance, often fluorescence tracking of protein dynamics and intracellular imaging and sensing require very small concentrations to resolve individual protein trafficking and to avoid perturbing the properties of live cells.

The images shown in Figure 3 indicate that dispersions of QDs photoligated with bis(LA)-ZW remain homogeneously dispersed and aggregate-free in PBS buffers (~20 mM) at pHs ranging from 2 to 14 for at least 5 months. Similarly, the fluorescence images shown in Figure 3b,c indicate that these dispersions stay stable for several months of storage at 4 °C in 50% and 100% cell growth media, and in the presence of 1 and 2 M NaCl. Similarly, we observed that dispersions of QDs photoligated with bis(LA)-ZW remain homogeneous and highly fluorescent in the presence of 10 mM glutathione for 2 weeks. A loss of emission (by ~90%) is measured after 3 weeks, but the dispersion stayed homogeneous and aggregate-free for up to 2 months. The stability of dispersions at nanomolar concentrations under daylight and at room temperature exposure was determined for three sets of QDs photoligated with bis(LA)-ZW, LA-PEG-OCH_3, and LA-ZW; the last two provided control samples. All samples were purified from excess free ligands by applying three rounds of concentration/dilution using a membrane filtration device from Millipore as mentioned above.

We tracked the colloidal stability of all three dispersions to check for turbidity buildup and monitored changes in the fluorescent intensity by collecting the emission spectra at different storage intervals. Data show that QDs photoligated with bis(LA)-ZW stay homogeneous and aggregate-free for all three concentrations, 10, 50, and 100 nM, after several months (samples were tracked for up to 6 months). The fluorescence intensity was also retained for at least 11 weeks with marginal changes observed for the 50 and 100 nM dispersions (Figure 4). Nonetheless, the 10 nM QD dispersions exhibited a loss in fluorescence after 3 weeks of storage (Figure 4); typically a loss of ~20% was measured after 3 weeks of storage, but the sample remained fluorescent for ~2 months. In comparison, the fluorescence intensity of QD prepared with LA-PEG-OCH_3 and LA-ZW ligands progressively decreased with time accompanied by aggregation buildup for LA-ZW-QDs after 3 weeks of storage (see the Supporting Information, Figure S6). For instance, the fluorescent intensity of 50 nM QDs photoligated with LA-PEG-OCH_3 dropped by ~50% after 1 week and ~90% after 2 weeks and became essentially nonemitting after 3 weeks. Dispersions of QDs photoligated with LA-ZW decreased by ~40% after 1 week and 60% after 2 weeks, but fluorescence persisted after 2 months, though macroscopic aggregation took place (see the Supporting Information, Figure S6).

These results indicate that the colloidal stability of QDs capped with DHLA-based ligands, though much stronger than that of monodentate (thiol and amine-modified) ligands, is

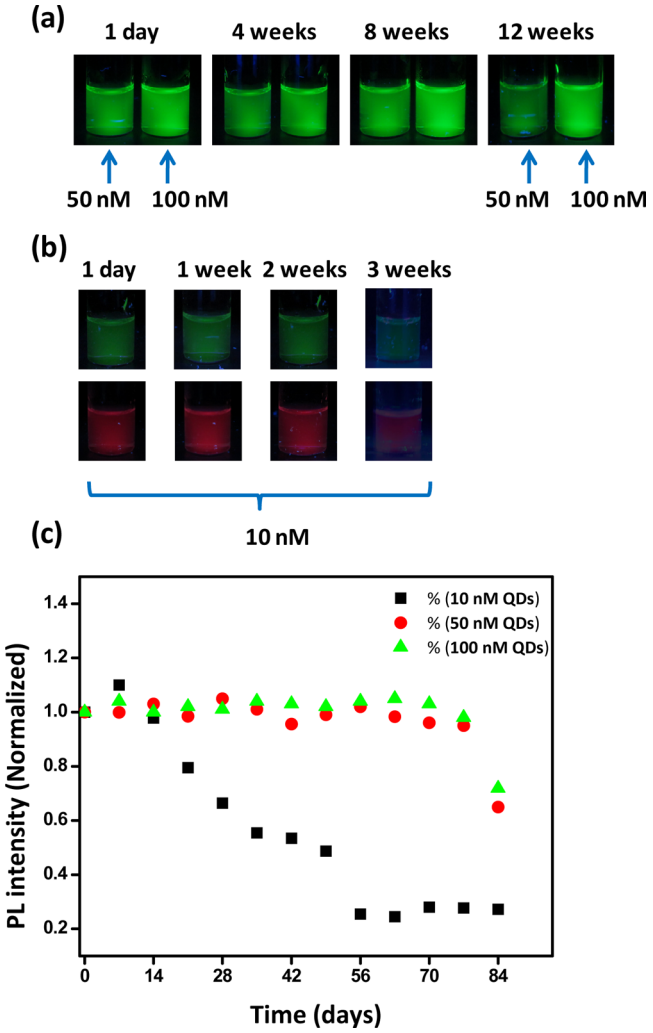

Figure 4. (a, b) Fluorescence images for a few dispersions (green- and red-emitting QDs) taken after the given storage times. Samples were stored at room temperature and under daylight exposure. (c) Plot of PL intensity versus storage time for dispersions of green-emitting QDs photoligated with bis(LA)-ZW at the indicated molar concentrations. The signal was normalized to the value at day 1. Similar data were collected for the red-emitting QDs.

weaker than those exhibited by nanocrystals capped with higher coordination ligands such as bis(DHLA)-modified ligands shown here and in ref 39. We should note that our data also indicate that dispersions of CdSe-ZnS QDs photoligated with LA-PEG ligands are more stable than those reported in ref 19, where a complete loss of fluorescence was measured for DHLA-PEG-capped CdSe-CdS QDs after 15 h of storage for similar concentrations (less than 100 nM) under ambient conditions. The poorer long-term stability for those samples may be attributed to the use of CdS-overcoated QDs. Thiol capping of Cd-rich surfaces is known to strongly affect their emission, much more than those of CdSe-ZnS QDs.

Regardless of the nature of the overcoating shell, our stability data confirm the ability of our ligand design to provide hydrophilic QDs that exhibit great colloidal stability when stored at nanomolar concentration at ambient temperature and daylight conditions. The improved stability is permitted by the higher coordination of the bis(LA)-ZW ligands onto the QD surface, which promotes stronger affinity between ligand and nanocrystal and shifts the equilibrium of bound versus unbound

dx.doi.org/10.1021/ja405010v | J. Am. Chem. Soc. 2013, 135, 13786−13795

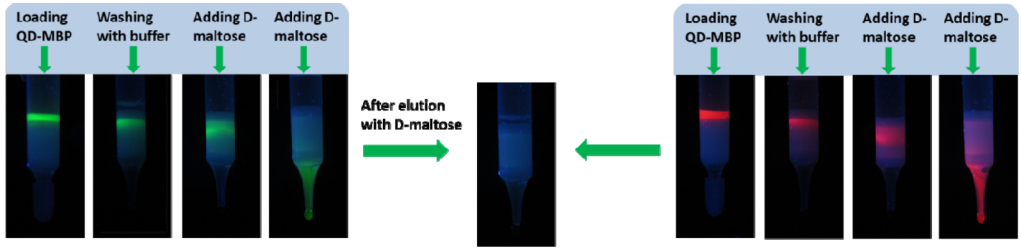

Figure 5. Assay testing the biological activity of the QD-MBP-His conjugates. Conjugates tightly bind onto amylose gel and are released by the addition of soluble maltose. Two colors of QDs photoligated with bis(LA)-ZW ligand were tested, green emitting (λ_{em} = 540, left) and red-emitting (λ_{em} = 624 nm, right).

ligands to much lower reagent concentrations. These results have profound implications on the use of such fluorescent QD platforms, as long-term stability of the nanocrystals in biological media at nanomolar concentrations is required.

The compactness of the QDs capped with bis(LA)-ZW was confirmed using dynamic light scattering measurements, which showed that the hydrodynamic radius of green-emitting nanocrystals was 5.3 nm, with a marginal increase in comparison to the native TOPO/TOPO-QDs in toluene (see the Supporting Information for more details). Further confirmation of the compactness of the zwitterion-modified ligands was provided by testing the ability of these QDs to self-assemble with MBP and mCherry expressing terminal polyhistidine tags, where direct coordination of the imidazole groups onto the Zn-rich surface is required (see below).

Protein Conjugation. Conjugation of nanoparticles to polyhistidine (His_n)-tagged proteins and peptides, promoted by metal-affinity interactions, has been explored by several groups, due to the ease of implementation and the fact that his-tagged biomolecules are ubiquitous.[49−52] Indeed, proteins are routinely expressed with a terminal polyhistidine tag to allow postpreparation purification (of the protein from undesired compounds) via affinity chromatography using Ni-NTA gel columns. We have demonstrated that the conjugation of CdSe-ZnS QDs with His-tagged proteins requires use of small capping ligands to promote the nanocrystal hydrophilicity, unless an extension linker is genetically inserted between the terminus and the His tag or the Ni-NTA group is laterally grafted onto the QD surface ligands.[52−55] In earlier reports, we used DHLA-QDs for conjugation to proteins, but this ligand provides QD stability only under basic buffer conditions.[35,51,56] Recently, we have shown that compact ligands DHLA-ZW and DHLA-TEG-ZW are better alternatives to DHLA, as they provide QDs that are colloidally stable over a broader pH range and can allow QD-biomolecule self-assembly under both acidic and basic conditions.[46]

Here, we extended those findings to QDs photoligated with bis(LA)-ZW ligands and tested metal-affinity interactions with two different proteins: (1) coupling to MBP-His_7 protein was tested using affinity chromatography to amylose gel followed by release with soluble maltose;[46] (2) self-assembly between QDs and mCherry-His_6 fluorescent protein, where the QD-mCherry assembly was confirmed using fluorescence resonance energy transfer (FRET). Figure 5 shows that dispersions of self-assembled QD-MPB conjugates (prepared with a valence of 12:1, see the Experimental Section for more details) tightly bind onto the top of an amylose column and stay bound even after several washes with buffer, as indicated by the fluorescent band generated by UV excitation of the immobilized QD-MBP conjugates using a hand-held UV lamp (λ_{exc} = 365 nm). Addition of 20 mM D-maltose solution led to immediate release of these conjugates, which were then collected in an Eppendorf tube (see Figure 5). The release was driven by the fact that added maltose (being the substrate for the protein) successfully competes with amylose for binding to MBP. This test was successfully applied to different sets of QDs photoligated with the same bis(LA)-ZW ligands. It clearly proved that QD-MBP conjugates were formed and that the conjugates maintained the protein biological activity.

In the second example, we self-assembled these QDs with increasing concentration of mCherry-His_6, corresponding to a protein-to-QD molar ratio (or conjugate valence) ranging from 3 to 15 (see schematics in Figure 6a). The concentration of the proteins in the solution was estimated using the extinction coefficients of mCherry (66314 M^{-1} cm^{-1} at λ = 586 nm) and the QDs (8.37×10^{-5} M^{-1} cm^{-1} at λ = 350 nm).[57,58] The absorption spectra in Figure 6b show an increasing contribution from mCherry to the measured absorption at 595−610 nm that tracks the amount of protein added. Similarly, the composite fluorescence spectra collected from these samples (excitation at 400 nm) show distinct contributions from the QDs and protein, coupled with a progressive reduction in QD emission and an increase in the mCherry signal (see Figure 6c). A control experiment using solutions of mCherry at the equivalent concentrations provided only a small signal, much smaller than the mCherry contribution to the spectra collected from the conjugates (see Figure 6c). The low direct excitation emission results from the fact that 400 nm is within the absorption valley of the protein and indicates that all the mCherry signal measured for the conjugate is essentially due to resonance enhancement promoted by FRET interactions.[57,59,60] Figure 6d shows visual evidence of the changes in the PL emission due to FRET. An extremely weak emission is generated from the tube containing mCherry alone when excited at 365 nm using a hand-held UV lamp. In contrast, higher emission combined with a progressive shift from green to orange can be seen from the samples with increasing molar concentration of mCherry (or higher conjugate valence).

Analysis of the fluorescence data is complicated by the fact that on conjugation to His-tagged proteins the QD emission often increases with the conjugate valence, as reported for DHLA-capped QDs.[35,51] A similar trend is observed for the present conjugates using QDs photoligated with bis(LA)-ZW or with LA-ZW. For instance, an increase of ∼50% was measured for MBP-His_7 conjugates at an average valence of 6 (see the Supporting Information). We thus need to take this into account when extracting quantitative information from the fluorescence data with QD-mCherry conjugates. For this we used the overall trend in the PL enhancement measured for the

dx.doi.org/10.1021/ja405010v | J. Am. Chem. Soc. 2013, 135, 13786−13795

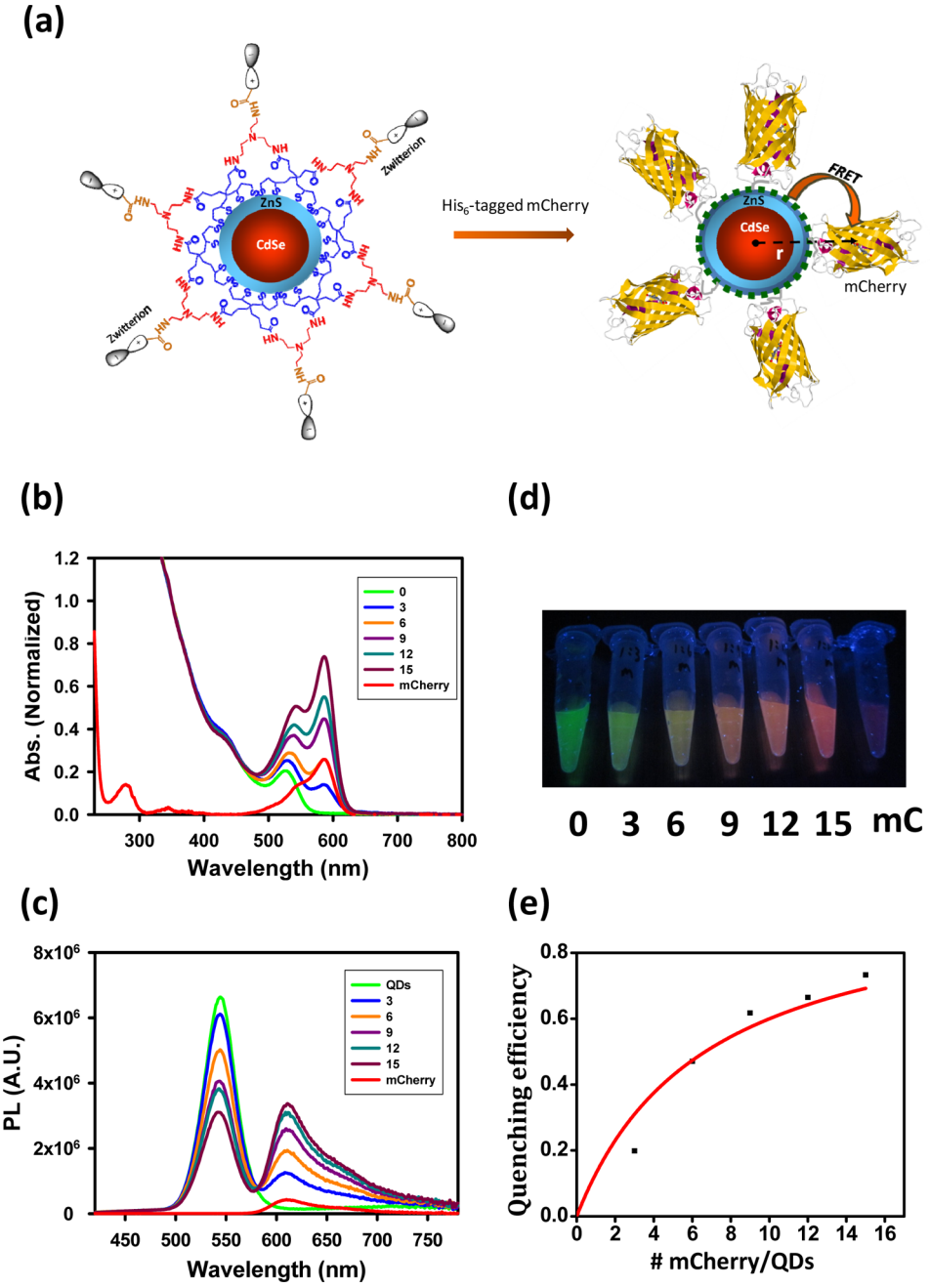

Figure 6. (a) Schematic representation of the metal−histidine conjugation. The zwitterion capping layer is represented by the green shell around the inorganic core in the conjugates. QD, ligand, and protein are not represented to scale. UV−vis absorption (b) and PL spectra (c) of QDs self-assembled with indicated protein-to-QD molar ratios ranging from 3 to 15. Also provided are spectra from control samples of mCherry. (d) Fluorescence image from Eppendorf tubes containing QDs and QD-mCherry conjugates with different molar ratios of mCherry per QD, along with mCherry alone. (e) Plot of the FRET efficiency vs amounts of mCherry per conjugate extracted from the emission spectra shown in (c).

QD-MBP-His_7 assemblies (shown in the Supporting Information, Figure S7).[51]

We first extracted values for the QD PL quenching efficiencies from the deconvoluted emission spectra at each valence using the above corrected QD spectra and the formula[61]

$$E_n = \frac{F_D - F_{DA}}{F_D} \quad (1)$$

where F_D and F_{DA} are the fluorescence intensities collected from the donor alone (here we used the value measured for the QD-MBP conjugates) and the donor in the presence of the mCherry acceptors, respectively. The fluorescence data were combined with the Förster dipole−dipole formalism to extract information about the self-assembled QD-mCherry conjugates.

The dependence of the experimental efficiencies versus valence, n, was compared to the expression of the FRET efficiency developed using a combination of the Förster dipole−dipole formalism and a centrosymmetric conjugate configuration made of one central donor and n acceptors arrayed at a fixed separation distance, E_n, given by[62]

dx.doi.org/10.1021/ja405010v | J. Am. Chem. Soc. 2013, 135, 13786−13795

$$E_n = \frac{nR_0^6}{nR_0^6 + r^6} \quad (2)$$

where r is the separation distance from the center of the donor to the center of the acceptor and R_0 is the Förster radius corresponding to $E_{n=1} = 0.5$, given by[61]

$$R_0 = (9.78 \times 10^3)(n_D^{-4}\kappa_p^2 Q_D I)^{1/6} \quad (3)$$

R_0 (expressed in Å) depends on the PL quantum yield of the donor, Q_D, the refractive index of the medium, n_D, Avogadro's number, N_A, the dipole orientation parameter, κ_p, and the spectral overlap integral, I. We used a value of $\kappa_p^2 = {}^2/_3$ for the orientation factor, justified for our present configuration.[60] I is extracted from integration (over all wavelengths) of the spectral overlap function, $J(\lambda) = PL_{D\text{-}corr}(\lambda) \times \lambda^4 \times \varepsilon_A$; where $PL_{D\text{-}corr}$ and ε_A designate the normalized fluorescence spectrum of the donor and the extinction coefficient spectrum of the acceptor, respectively. Using the protein structure retrieved from the protein data bank (PDB), a QD radius of ∼32 Å,[14] a distance between QD-surface and the location of the fluorophore within the mCherry β barrel of ∼28 Å, a Q_D value ∼19%, and the assumption that the histidine tag contribution to the lateral extension is rather small, we estimate an experimental r value of ∼60 Å.

Using this information, we estimated the number of proteins assembled per QD for the above mCherry with molar concentrations to be 3, 5, 9, 12, and 14, respectively; the corresponding optimal fit using eq 2 to the experimental data is shown in Figure 6e. These values are in relatively good agreement with the expected values for the molar ratio of protein-to-QD corresponding to the concentration used.

Covalent Coupling to Target Molecules. Covalent coupling of amine- or carboxy-QDs, initially prepared by introducing a small fraction of bis(LA)-NH_2 or bis(LA)-COOH along with bis(LA)-ZW during the photoligation step, can be carried out using a conventional EDC (1-ethyl-3-(3-dimethylaminopropyl)carbodiimide) condensation reaction. Indeed, we applied this method to couple amine-QDs, prepared using a 10% molar fraction of aminated bis(LA) ligands, to NHS-activated Sulfo-Cy3 dye. We also coupled carboxy-QDs to folic acid using EDC coupling (data not shown). Effective dye coupling has been verified using a combination of gel electrophoresis and fluorescence quenching spectroscopy.[18] Gel electrophoresis data indicate a change in the mobility shift of the QDs following covalent attachment with Cy3, while fluorescence measurements showed a pronounced quenching of QD PL emission, coupled with an increase in the dye contribution (compared to dye only solution). Additional details are provided in the Supporting Information (e.g., Figure S9).

CONCLUSION

We have designed and prepared a new set of metal and semiconductor coordinating ligands, which combine a multithiol anchor made of two lipoic acid functions and a zwitterion group. We combined this ligand with a new photoligation strategy recently reported by us to stabilize CdSe-ZnS QDs in buffer media over a broad range of conditions. In particular, we found that the resulting QDs exhibit great colloidal stability over a broad pH range, to added electrolytes, and in the presence of growth media and added reducing agent. Furthermore, by increasing the ligand coordination (using bis(LA) instead of one LA) we found that the QDs were colloidally stable at nanomolar concentrations and under ambient conditions (room temperature and white light exposure). This is particularly promising for fluorescent labeling in biology, such as intracellular imaging and sensing, where very small concentrations (nanomolar or so) are often required.

The compact nature of the zwitterion ligand further permitted the use of metal−histidine self-assembly between QDs photoligated with bis(LA)-ZW and two different His-tagged proteins, maltose binding protein and the fluorescent mCherry protein. Self-assembly with the latter permitted resonance energy transfer interactions to be tested with these assemblies. The remarkable colloidal stability of QDs capped with these multicoordinating and compact zwitterion ligands, combined with the compatibility with metal−histidine conjugation, bodes well for a variety of applications ranging from protein tracking and ligand−receptor binding to intracellular sensing using energy transfer interactions. We are presently exploiting this system to test intracellular uptake of QD cargos by live cells. We should also add that such ligand design can be applied to other metal-rich nanostructures, including Au and Ag nanoparticles and nanorods.

ASSOCIATED CONTENT

Supporting Information

Text and figures giving additional experimental details, including MBP expression, covalent conjugation, ^{1}H NMR data, ESI-MS spectra of zwitterion compounds, DLS, daylight stability data of QD dispersions, gel electrophoresis data, and PL spectra of conjugates. This material is available free of charge via the Internet at http://pubs.acs.org.

AUTHOR INFORMATION

Corresponding Author

mattoussi@chem.fsu.edu.

Notes

The authors declare no competing financial interest.

ACKNOWLEDGMENTS

We thank FSU and the National Science Foundation (NSF-CHE, No. 1058957) for financial support. We also thank Tommaso Avellini, Anshika Kapur, Wentao Wang, and Fadi Aldeek for helpful discussions and assistance. We thank Mike Davidson and Professor Tim A. Cross at FSU for kindly providing us with the MBP and mCherry plasmids.

REFERENCES

(1) Bruchez, M.; Moronne, M.; Gin, P.; Weiss, S.; Alivisatos, A. P. *Science* **1998**, *281*, 2013.
(2) Medintz, I. L.; Uyeda, H. T.; Goldman, E. R.; Mattoussi, H. *Nat. Mater.* **2005**, *4*, 435.
(3) Pinaud, F.; Clarke, S.; Sittner, A.; Dahan, M. *Nat. Methods* **2010**, *7*, 275.
(4) Mattoussi, H.; Palui, G.; Na, H. B. *Adv. Drug Delivery Rev.* **2012**, *64*, 138.
(5) Zrazhevskiy, P.; Sena, M.; Gao, X. H. *Chem. Soc. Rev.* **2010**, *39*, 4326.
(6) Talapin, D. V.; Lee, J. S.; Kovalenko, M. V.; Shevchenko, E. V. *Chem. Rev.* **2010**, *110*, 389.
(7) Resch-Genger, U.; Grabolle, M.; Cavaliere-Jaricot, S.; Nitschke, R.; Nann, T. *Nat. Methods* **2008**, *5*, 763.
(8) Murray, C. B.; Norris, D. J.; Bawendi, M. G. *J. Am. Chem. Soc.* **1993**, *115*, 8706.
(9) Peng, Z. A.; Peng, X. G. *J. Am. Chem. Soc.* **2001**, *123*, 183.

(10) Reiss, P.; Protiere, M.; Li, L. *Small* **2009**, *5*, 154.
(11) Reiss, P.; Bleuse, J.; Pron, A. *Nano Lett.* **2002**, *2*, 781.
(12) Kovalenko, M. V.; Bodnarchuk, M. I.; Zaumseil, J.; Lee, J. S.; Talapin, D. V. *J. Am. Chem. Soc.* **2010**, *132*, 10085.
(13) Clapp, A. R.; Goldman, E. R.; Mattoussi, H. *Nat. Protoc.* **2006**, *1*, 1258.
(14) Mattoussi, H.; Cumming, A. W.; Murray, C. B.; Bawendi, M. G.; Ober, R. *Phys. Rev. B* **1998**, *58*, 7850.
(15) Dabbousi, B. O.; RodriguezViejo, J.; Mikulec, F. V.; Heine, J. R.; Mattoussi, H.; Ober, R.; Jensen, K. F.; Bawendi, M. G. *J. Phys. Chem. B* **1997**, *101*, 9463.
(16) Murray, C. B.; C., R. K.; Bawendi, M. G. *Annu. Rev. Mater. Sci.* **2000**, *30*, 545.
(17) Hines, M. A.; Guyot-Sionnest, P. *J. Phys. Chem.* **1996**, *100*, 468.
(18) Susumu, K.; Uyeda, H. T.; Medintz, I. L.; Pons, T.; Delehanty, J. B.; Mattoussi, H. *J. Am. Chem. Soc.* **2007**, *129*, 13987.
(19) Liu, W. H.; Greytak, A. B.; Lee, J.; Wong, C. R.; Park, J.; Marshall, L. F.; Jiang, W.; Curtin, P. N.; Ting, A. Y.; Nocera, D. G.; Fukumura, D.; Jain, R. K.; Bawendi, M. G. *J. Am. Chem. Soc.* **2010**, *132*, 472.
(20) Yildiz, I.; Deniz, E.; McCaughan, B.; Cruickshank, S. F.; Callan, J. F.; Raymo, F. M. *Langmuir* **2010**, *26*, 11503.
(21) Dubertret, B.; Skourides, P.; Norris, D. J.; Noireaux, V.; Brivanlou, A. H.; Libchaber, A. *Science* **2002**, *298*, 1759.
(22) Pellegrino, T.; Manna, L.; Kudera, S.; Liedl, T.; Koktysh, D.; Rogach, A. L.; Keller, S.; Radler, J.; Natile, G.; Parak, W. J. *Nano Lett.* **2004**, *4*, 703.
(23) Yu, W. W.; Chang, E.; Falkner, J. C.; Zhang, J. Y.; Al-Somali, A. M.; Sayes, C. M.; Johns, J.; Drezek, R.; Colvin, V. L. *J. Am. Chem. Soc.* **2007**, *129*, 2871.
(24) Giovanelli, E.; Muro, E.; Sitbon, G.; Hanafi, M.; Pons, T.; Dubertret, B.; Lequeux, N. *Langmuir* **2012**, *28*, 15177.
(25) Chen, Y.; Thakar, R.; Snee, P. T. *J. Am. Chem. Soc.* **2008**, *130*, 3744.
(26) Snee, P. T.; Somers, R. C.; Nair, G.; Zimmer, J. P.; Bawendi, M. G.; Nocera, D. G. *J. Am. Chem. Soc.* **2006**, *128*, 13320.
(27) Schmidtke, C.; Lange, H.; Tran, H.; Ostermann, J.; Kloust, H.; Bastús, N. G.; Merkl, J.-P.; Thomsen, C.; Weller, H. *J. Phys. Chem. C* **2013**, *117*, 8570.
(28) Palui, G.; Na, H. B.; Mattoussi, H. *Langmuir* **2012**, *28*, 2761.
(29) Liu, W.; Howarth, M.; Greytak, A. B.; Zheng, Y.; Nocera, D. G.; Ting, A. Y.; Bawendi, M. G. *J. Am. Chem. Soc.* **2008**, *130*, 1274.
(30) Liu, D.; Snee, P. T. *ACS Nano* **2011**, *5*, 546.
(31) Kim, C. S.; Tonga, G. Y.; Solfiell, D.; Rotello, V. M. *Adv. Drug Delivery Rev.* **2013**, *65*, 93.
(32) Muro, E.; Pons, T.; Lequeux, N.; Fragola, A.; Sanson, N.; Lenkei, Z.; Dubertret, B. *J. Am. Chem. Soc.* **2010**, *132*, 4556.
(33) Smith, A. M.; Nie, S. *J. Visualized Exp.* **2012**, DOI: 10.3791/4236 .
(34) Medintz, I. L.; Stewart, M. H.; Trammell, S. A.; Susumu, K.; Delehanty, J. B.; Mei, B. C.; Melinger, J. S.; Blanco-Canosa, J. B.; Dawson, P. E.; Mattoussi, H. *Nat. Mater.* **2010**, *9*, 676.
(35) Mattoussi, H.; Mauro, J. M.; Goldman, E. R.; Anderson, G. P.; Sundar, V. C.; Mikulec, F. V.; Bawendi, M. G. *J. Am. Chem. Soc.* **2000**, *122*, 12142.
(36) Pons, T.; Uyeda, H. T.; Medintz, I. L.; Mattoussi, H. *J. Phys. Chem. B* **2006**, *110*, 20308.
(37) Liu, W.; Choi, H. S.; Zimmer, J. P.; Tanaka, E.; Frangioni, J. V.; Bawendi, M. *J. Am. Chem. Soc.* **2007**, *129*, 14530.
(38) Uyeda, H. T.; Medintz, I. L.; Jaiswal, J. K.; Simon, S. M.; Mattoussi, H. *J. Am. Chem. Soc.* **2005**, *127*, 3870.
(39) Stewart, M. H.; Susumu, K.; Mei, B. C.; Medintz, I. L.; Delehanty, J. B.; Blanco-Canosa, J. B.; Dawson, P. E.; Mattoussi, H. *J. Am. Chem. Soc.* **2010**, *132*, 9804.
(40) Yildiz, I.; McCaughan, B.; Cruickshank, S. F.; Callan, J. F.; Raymo, F. M. *Langmuir* **2009**, *25*, 7090.
(41) Susumu, K.; Oh, E.; Delehanty, J. B.; Blanco-Canosa, J. B.; Johnson, B. J.; Jain, V.; Hervey, W. J.; Algar, W. R.; Boeneman, K.; Dawson, P. E.; Medintz, I. L. *J. Am. Chem. Soc.* **2011**, *133*, 9480.
(42) Park, J.; Nam, J.; Won, N.; Jin, H.; Jung, S.; Jung, S.; Cho, S. H.; Kim, S. *Adv. Funct. Mater.* **2011**, *21*, 1558.
(43) Palui, G.; Avellini, T.; Zhan, N.; Pan, F.; Gray, D.; Alabugin, I.; Mattoussi, H. *J. Am. Chem. Soc.* **2012**, *134*, 16370.
(44) Yu, W. W.; Peng, X. G. *Angew. Chem., Int. Ed.* **2002**, *41*, 2368.
(45) Tamang, S.; Beaune, G.; Texier, I.; Reiss, P. *ACS Nano* **2011**, *5*, 9392.
(46) Zhan, N.; Palui, G.; Grise, H.; Tang, H.; Alabugin, I.; Mattoussi, H. *ACS Appl. Mater. Interfaces* **2013**, *5*, 2861.
(47) Shi, Z.-Z.; Osei-Frimpong, J.; Kala, G.; Kala, S. V.; Barrios, R. J.; Habib, G. M.; Lukin, D. J.; Danney, C. M.; Matzuk, M. M.; Lieberman, M. W. *Proc. Natl. Acad. Sci. U.S.A.* **2000**, *97*, 5101.
(48) Cooper, A. J. L.; Kristal, B. S. *Biol. Chem.* **1997**, *378*, 793.
(49) Dif, A.; Boulmedais, F.; Pinot, M.; Roullier, V.; Baudy-Floc'h, M.; Coquelle, F. M.; Clarke, S.; Neveu, P.; Vignaux, F.; Le Borgne, R.; Dahan, M.; Gueroui, Z.; Marchi-Artzner, V. *J. Am. Chem. Soc.* **2009**, *131*, 14738.
(50) Petryayeva, E.; Algar, W. R.; Krull, U. J. *Langmuir* **2013**, *29*, 977.
(51) Medintz, I. L.; Clapp, A. R.; Mattoussi, H.; Goldman, E. R.; Fisher, B.; Mauro, J. M. *Nat. Mater.* **2003**, *2*, 630.
(52) Boeneman, K.; Mei, B. C.; Dennis, A. M.; Bao, G.; Deschamps, J. R.; Mattoussi, H.; Medintz, I. L. *J. Am. Chem. Soc.* **2009**, *131*, 3828.
(53) Roullier, V.; Clarke, S.; You, C.; Pinaud, F.; Gouzer, G.; Schaible, D.; Marchi-Artzner, V.; Piehler, J.; Dahan, M. *Nano Lett.* **2009**, *9*, 1228.
(54) Smith, A. M.; Nie, S. *J. Am. Chem. Soc.* **2008**, *130*, 11278.
(55) Bae, P. K.; Kim, K. N.; Lee, S. J.; Chang, H. J.; Lee, C. K.; Park, J. K. *Biomaterials* **2009**, *30*, 836.
(56) Dennis, A. M.; Sotto, D. C.; Mei, B. C.; Medintz, I. L.; Mattoussi, H.; Bao, G. *Bioconjugate Chem.* **2010**, *21*, 1160.
(57) Dennis, A. M.; Bao, G. *Nano Lett.* **2008**, *8*, 1439.
(58) Leatherdale, C. A.; Woo, W. K.; Mikulec, F. V.; Bawendi, M. G. *J. Phys. Chem. B* **2002**, *106*, 7619.
(59) Medintz, I. L.; Pons, T.; Susumu, K.; Boeneman, K.; Dennis, A. M.; Farrell, D.; Deschamps, J. R.; Melinger, J. S.; Bao, G.; Mattoussi, H. *J. Phys. Chem. C* **2009**, *113*, 18552.
(60) Medintz, I. L.; Mattoussi, H. *Phys. Chem. Chem. Phys.* **2009**, *11*, 17.
(61) Lakowicz, J. R. *Principles of fluorescence spectroscopy*, 3rd ed.; Springer: New York, 2006.
(62) Clapp, A. R.; Medintz, I. L.; Mauro, J. M.; Fisher, B. R.; Bawendi, M. G.; Mattoussi, H. *J. Am. Chem. Soc.* **2004**, *126*, 301.